nature physics

LETTERS

PUBLISHED ONLINE: 5 MAY 2013 | DOI: 10.1038/NPHYS2614

A cold-atom random laser

Q. Baudouin, N. Mercadier†, V. Guarrera†, W. Guerin and R. Kaiser*

In conventional lasers optical cavities are used to provide feedback to gain media. Mirrorless lasers can be built by using disordered structures to induce multiple scattering, which increases the path length in the medium, providing the necessary feedback[1]. Interestingly, light or microwave amplification by stimulated emission also occurs naturally in stellar gases[2–4] and planetary atmospheres[5,6]. The possibility of additional scattering-induced feedback[4,7]—random lasing[8–14]—could explain the unusual properties of some space masers[15]. Here, we report experimental evidence of random lasing in a controlled, cold atomic vapour, taking advantage of Raman gain. By tuning the gain frequency in the vicinity of a scattering resonance, we observe an enhancement of the light emission due to random lasing. The unique possibility to both control the experimental parameters and to model the microscopic response of our system provides an ideal test bench for better understanding natural lasing sources, in particular the role of resonant scattering feedback in astrophysical lasers.

A cloud of cold atoms constitutes a new medium to study random lasing[8–14], allowing a detailed microscopic understanding of gain and scattering. Multiple scattering of light in cold atoms has been extensively studied in the past[16,17]. Furthermore, quasi-continuous lasing with cold atoms as a gain medium, either placed inside optical cavities[18–21] or based on distributed feedback[22], has recently been demonstrated, illustrating the potential for a variety of gain mechanisms in a regime where optical coherence is limited by purely radiative decay channels. This is significantly different with respect to most random lasing devices, based on pulsed excitation of condensed-matter systems, where the relaxation rates of the optical coherence are several orders of magnitude faster than the decay of the excited state population. Long phase coherence times however allow for efficient feedback by resonant scattering, as expected in astrophysical lasers[4].

To combine sufficient gain and scattering while using only one atomic species, we take advantage of the multilevel structure of rubidium atoms, shown in Fig. 1a (D_2 line of ^{85}Rb, wavelength $\lambda = 780$ nm). Two-photon Raman gain is obtained by a population inversion between the two hyperfine ground states $|2\rangle$ and $|3\rangle$ sustained by optical pumping. A Raman laser drives the $|3\rangle \rightarrow |2'\rangle$ transition with a large detuning Δ, so that atoms can be transferred into the $|2\rangle$ state by stimulated emission. Scattering required for random lasing is provided by the $|2\rangle \rightarrow |1'\rangle$ line, which is a closed transition efficient for multiple scattering. Both Raman gain and scattering can occur at the same frequency (that is, for the same photons) by an appropriate choice of the Raman detuning $\Delta = -4.8\Gamma$, determined by the hyperfine splitting between the $|1'\rangle$ and $|2'\rangle$ states ($\Gamma/2\pi = 6$ MHz is the linewidth of the transition). We thus tune the Raman laser to the vicinity of this condition and define the detuning $\delta = \Delta + 4.8\Gamma$ as the relevant parameter (Fig. 1a). This scheme takes advantage of the selection rules, which forbid electric dipole transitions between the states $|3\rangle$ and $|1'\rangle$, so that the $|1'\rangle$ level does not affect the Raman gain.

For a given amount of gain and scattering, the threshold of random lasing is determined by a critical minimum size of the sample[1]. In our case, gain and scattering are provided by the same atoms and depend on the atomic density n. We have shown[23–25] that the critical parameter defining the random-laser threshold is the on-resonance optical thickness b_0, defined for a homogeneous cloud of radius R as $b_0 = 2n\sigma_{34'}R$, with $\sigma_{34'}$ being the on-resonance scattering cross-section for the $|3\rangle \rightarrow |4'\rangle$ transition (used to measure b_0; see Methods and Supplementary Fig. S1). Moreover, its critical value can be computed from the atomic polarizability alone (see Supplementary Information).

Our sample consists of a cloud of cold ^{85}Rb atoms collected in a magneto-optical trap. A controlled compression period provides a variable optical thickness b_0 with a constant number of trapped atoms (see Methods). We then switch off all lasers and magnetic field gradients 1 ms before applying strong counterpropagating Raman beams (intensity $I_{Ra} = 4.25$ mW cm^{-2} per beam with crossed linear polarizations) tuned around $\delta \sim 0$. In addition, we use an optical-pumping laser tuned slightly below the $|2\rangle \rightarrow |3'\rangle$ transition to sustain a steady-state population inversion between the two hyperfine levels involved in our scheme. The relative intensity between the two external lasers allows us to adjust the relative populations, and thus to tune continuously from a sample with large gain and no scattering (with all atoms in the $|3\rangle$ state) to a situation without gain and with large scattering on the $|2\rangle \rightarrow |1'\rangle$ line (with all atoms in the $|2\rangle$ state). Note that with the chosen detunings, these lasers operate in the single scattering regime. The data presented here have been obtained with an optical-pumping intensity $I_{OP} = 2.9$ mW cm^{-2}, ensuring a small population inversion.

In random lasers, there is not any privileged emission direction that allows one to spatially separate the random-laser light from amplified spontaneous emission and scattering from the pump beam, which is usually much stronger than the random-laser emission itself. In our system, however, the $|2\rangle \rightarrow |1'\rangle$ transition does not scatter light from the two external lasers. The random-laser line thus has a strength comparable to the one of the other involved transition and the signature of random lasing can be obtained by the detection of the total emitted light from the sample, which we collect with a solid angle of 10^{-2} sr at an angle of 40° with respect to the Raman beam axes (Fig. 1b). Figure 2 shows the measured fluorescence as the Raman laser frequency is swept through the region of interest, for different values of the optical thickness b_0 of the atomic cloud (see Methods). We stress that for these measurements we vary b_0 while keeping the atom number constant. Variations in the fluorescence can thus only be related to collective features.

The first signature of such a collective behaviour can be seen in a regime of negligible scattering, far from the $|2\rangle \rightarrow |1'\rangle$

Institut Non Linéaire de Nice, CNRS, Université de Nice Sophia-Antipolis, 1361 route des Lucioles, 06560 Valbonne, France. †Present addresses: Saint-Gobain Recherche, 39 quai Lucien Lefranc, 93303 Aubervilliers, France (N.M.); LNE-SYRTE, Observatoire de Paris, CNRS, UPMC, 61 avenue de l'Observatoire, 75014 Paris, France (V.G.). *e-mail: robin.kaiser@inln.cnrs.fr

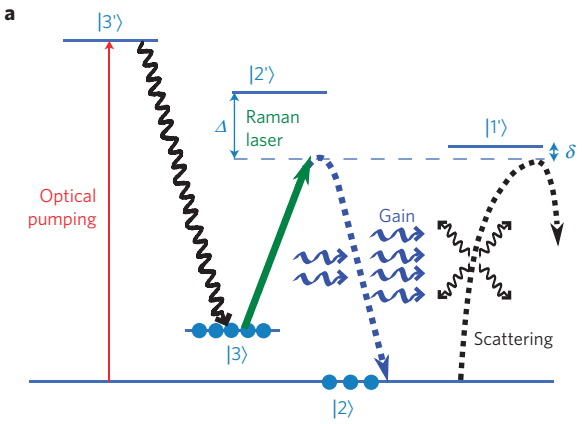

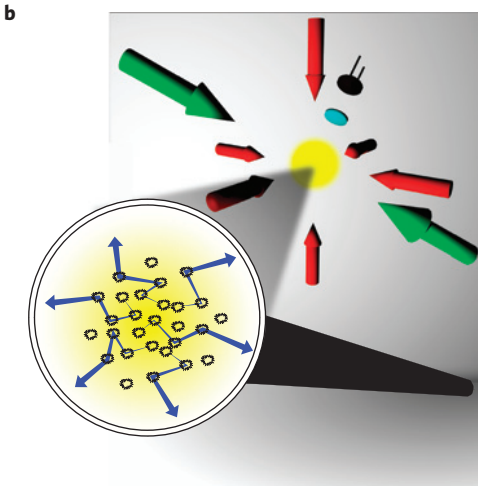

Figure 1 | Working principle of the random laser. a, Atomic transitions of the D_2 line of ^{85}Rb (at $\lambda = 780.24$ nm) used to create random lasing in cold atoms. The two hyperfine ground states are $|2\rangle = |F = 2\rangle$ and $|3'\rangle = |F' = 3\rangle$, separated by 3 GHz. Similarly, the involved hyperfine excited states are the states $|F' = 1, 2, 3\rangle$ denoted $|1'\rangle$, $|2'\rangle$ and $|3'\rangle$ with splittings of a few tens of megahertz. Optical pumping creates a population inversion between $|2\rangle$ and $|3\rangle$. This allows us to create Raman gain by applying a laser with a detuning Δ from the $|3\rangle \rightarrow |2'\rangle$ transition. The gain frequency has a detuning δ from the closed $|2\rangle \rightarrow |1'\rangle$ transition. Around $\delta \sim 0$, this transition provides efficient scattering. Random lasing can thus occur around this frequency. **b**, Schematic of the experiment. The cold-atom cloud (yellow sphere) is exposed to two Raman-laser beams (green) and six optical-pumping beams (red). Its fluorescence is collected by a lens and detected by a photodiode. Zoom-in: light (in blue) is scattered by atoms in the $|2\rangle$ state (black) and amplified by atoms in the $|3\rangle$ state (yellow background).

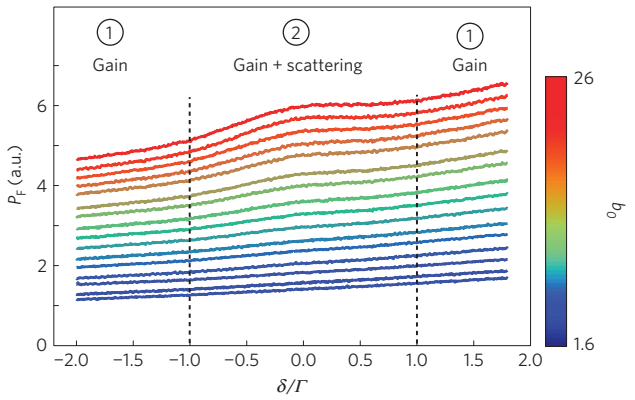

Figure 2 | Fluorescence measurement. Total fluorescence P_F as a function of the Raman laser detuning δ (in units of the linewidth Γ of the optical transition) recorded for optical thickness varying from $b_0 = 1.9$ to $b_0 = 26$. The number of atoms is kept constant at $N = 7 \times 10^8 \pm 12\%$. Two collective features are visible. In the wings (regions 1), the overall increase of the fluorescence with b_0 is due to amplified stimulated emission. Around $\delta \sim 0$ (region 2), an extra peak appears for large optical thickness. This enhanced light emission is due to the combination of Raman gain and multiple scattering provided by the $|2\rangle \rightarrow |1'\rangle$ transition and is thus a signature of random lasing.

transition (regions 1 of Fig. 2): amplified spontaneous emission (ASE) induces an overall increase of the fluorescence as a function of b_0. Photons from the Raman beam can indeed undergo a spontaneous Raman transition. The subsequent scattered light is then amplified by Raman gain produced by the surrounding atoms while leaving the sample with a ballistic path. The efficiency of this process is directly related to the optical thickness (see Supplementary Information). The ASE signal decreases as the Raman laser is detuned further away from the $|3\rangle \rightarrow |2'\rangle$ transition (located at $\delta = +4.8\Gamma$) because both the spontaneous (source contribution) and stimulated (gain contribution) Raman scattering rates decrease for larger detuning. Note that when tuning the Raman laser very close to the $|3\rangle \rightarrow |2'\rangle$ line, single-photon scattering dominates. As detailed in ref. 26, population redistribution is then responsible for the increase of fluorescence. This effect is negligible for the detunings considered here, and only gain can explain the observed features.

When the Raman laser is tuned close to $\delta = 0$ (region 2 of Fig. 2), the combination of gain and scattering gives rise to a random laser. It appears as an enhanced fluorescence bump that emerges as the optical thickness b_0 is increased. To better extract this signal, we fit the wings of the curves (regions 1) by adjustable slope and curvature and remove this ASE background. The remaining random-laser signal is a Gaussian peak, well centred at $\delta = 0$ (Fig. 3a), which thus comes from the scattering due to the $|2\rangle \rightarrow |1'\rangle$ transition. Therefore, the observed peak is due to the combination of gain and scattering. Moreover, although the signal consists of different emission lines, a threshold of the peak amplitude is clearly visible, with a change of slope at $b_0 = 6 \pm 1$ (Fig. 3b). This threshold is the signature of the occurrence of random lasing in our sample when the Raman beams are tuned around $\delta \sim 0$ and when $b_0 > 6$. We stress that varying the optical thickness acts simultaneously on the amount of gain and feedback provided by the medium. This is unusual in laser physics, where the threshold is most commonly defined as a critical pump power. In our case, increasing the optical-pumping intensity indeed increases the population inversion that provides gain, but simultaneously decreases the feedback, so that random lasing needs a fine tuning of the laser parameters.

Finally, we have exploited the possibility to perform *ab initio* theory by developing two simple models, one for ASE and the other for random lasing. Both are detailed in the Supplementary Information. Here, we describe briefly the random-lasing model. It consists of self-consistently coupling the atomic response, based on optical Bloch equations with additional scattering on the $|2\rangle \rightarrow |1'\rangle$ line, to a diffusion equation for the light scattered on the $|2\rangle \rightarrow |1'\rangle$ resonance. The optical Bloch equations allow us to compute the atomic polarizability and, including the additional scattering on the $|2\rangle \rightarrow |1'\rangle$ line, the mean-free path ℓ_{sc} and the gain length ℓ_g, including saturation effects due to the random laser intensity I_{RL} inside the sample. As in conventional laser theory, we look for a steady-state solution where gain exactly compensates losses. In the diffusive regime and taking into account only the diffuse mode with

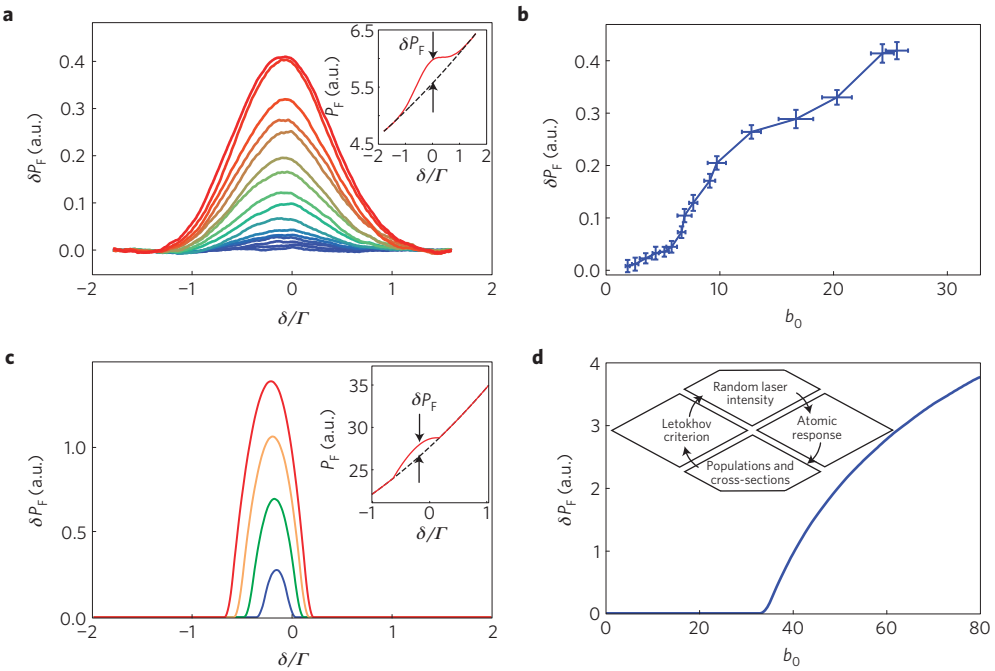

Figure 3 | Random laser emission around $\delta = 0$. a, Measured supplementary fluorescence δP_F due to random lasing as a function of the Raman laser detuning δ, measured for optical thickness varying from $b_0 = 1.9$ to $b_0 = 26$. The source data and the colour scale are the same as in Fig. 2, but the wings (regions 1 in Fig. 2) have been subtracted. The inset illustrates the fitting procedure. For clarity we also smoothed the data, corresponding to a detuning resolution of 0.3Γ. **b**, Measured amplitude of the peak due to random lasing. A threshold optical thickness is clearly visible at $b_0 \sim 6$. Vertical error bars correspond to the root mean squared noise on the data of Fig. 2 and horizontal error bars to shot-to-shot fluctuations of b_0. **c**, Computed supplementary fluorescence δP_F as a function of the detuning δ, using our self-consistent model for random lasing, neglecting the contribution from ASE, for four different optical thicknesses, $b_0 = 26$ (blue), $b_0 = 30$ (green), $b_0 = 34$ (orange) and $b_0 = 38$ (red). **d**, Maximum supplementary fluorescence δP_F computed from the self-consistent model for random lasing. Inset: principle of the model. The atomic response allows the computation of the threshold optical thickness following Letokhov's criterion[1,23]. Owing to saturation effects, this threshold depends on the random-laser intensity. Therefore, for each b_0, we find the random-laser intensity such that the computed threshold equals b_0, corresponding to a steady state (see Supplementary Information).

the longest lifetime, this condition is equivalent to Letokhov's result on the random-lasing threshold[1,23],

$$R_{cr} = \pi\sqrt{\frac{\ell_{sc}\ell_g}{3}} \qquad (1)$$

where R_{cr} is the critical sample size. As a consequence, for a given b_0, we find the value of I_{RL} such that equation (1) is fulfilled. Considering the absence of any free fitting parameter and the simplicity of our model, which neglects for instance the contribution of ASE, the experimental data and the computed values for the supplementary fluorescence show satisfactory qualitative agreement (Fig. 3). The quantitative discrepancies suggest the need for more involved models. Many ingredients could play a role in our experiment and have been neglected in our models, such as the inelastic spectrum of the emitted light, interference effects on light transport, light polarization, the Zeeman degeneracy of the involved atomic levels, the finite temperature, the inhomogeneous atomic density distribution, and cooperative effects[21,27]. The comparison between the experiment and new models including some of these effects will allow one to identify the most relevant ones and thus to better understand random-laser physics.

We have presented experimental evidence of combined gain and scattering of light in a cloud of cold atoms, demonstrating random lasing in a dilute vapour. This type of experiment, based on well-controlled atomic systems, with the possibility of *ab initio* calculations, will allow studying the role of interferences and cooperativity in random lasing[27–29]. The combined theoretical and experimental approach described in this work can also be applied to realistic atomic structures encountered in astrophysical systems and to test new detection schemes, based for instance on high-order photon correlations[30].

Methods

Sample preparation. In our experiment 6 counter-propagating trapping beams with a waist of 3.4 cm ($1/e^2$ radius of the intensity distribution) are used to load ^{85}Rb atoms from a background atomic vapour into a magneto-optical trap (MOT). The trapping beams are detuned by -3Γ from the $|3\rangle \rightarrow |4'\rangle$ hyperfine transition. To maintain the atomic populations in $|3\rangle$, we add 6 repumper beams tuned slightly below the $|2\rangle \rightarrow |3'\rangle$ transition. We can load between 10^8 and 10^{11} atoms by changing the background vapour pressure and the duration of the trap loading (from 10 to 500 ms). Once the atoms are trapped in the MOT, we perform a temporal dark-MOT stage by increasing the detuning of the trapping beams to -6Γ and by reducing the intensity of the repumper beams to a few per cent of their initial value. This leads to an increase of the spatial density and thus of the optical thickness b_0 of the cloud, without loss of atoms. By changing the duration of this compression stage, we are able to tune b_0 from 1.9 to 27, while keeping almost constant the total number of atoms, which, for the measurements presented here, is set to $7 \times 10^8 \pm 12\%$. The temperature is $T \sim 50\,\mu$K. The optical thickness b_0 is measured by a transmission spectrum with a small and weak probe beam on the $|3\rangle \rightarrow |4'\rangle$ transition[24]. The shot-to-shot fluctuations of b_0 (horizontal error bars in Fig. 3b) are evaluated by repeating the measurement five times.

Data acquisition. After the sample preparation, we switch off magnetic field gradients and trapping lasers and we expose the sample to two counterpropagating Raman beams with waists of 2.4 cm, intensities of 4.25 mW cm^{-2} each and linear orthogonal polarizations, and 3 pairs of counterpropagating optical pumping beams with waists of 3.4 cm, intensities of 0.48 mW cm^{-2} and σ^+/σ^- polarizations, each at a detuning of -3Γ from the $|2\rangle \rightarrow |3'\rangle$ transition. Note that the diameters of these lasers are large enough to ensure that their effective intensities on the atom cloud are independent from the chosen optical thickness. The Raman laser is obtained from a distributed-Bragg-reflector laser diode and is frequency-tuned by a double-pass acousto-optic modulator before it is amplified by two stages of saturated slave lasers. This system allows us to scan the frequency in a range up to 16Γ with intensity variations of only 0.1%.

The measuring procedure consists of scanning in 2 ms the Raman beam detuning δ from $-3,2\Gamma$ to $4,8\Gamma$ while a high-gain photodiode gathers the fluorescent emission of the cloud in a solid angle of $\sim 10^{-2}$ sr. The detected power is of the order of 0.4 nW. We checked that the direction of the sweep does not change the detected fluorescence, and that the duration of the sweep is short enough to avoid significant variations of b_0 during the measurements (<5%) and long enough to probe a quasi-steady state (the sweep rate is 4Γ ms^{-1}). We averaged over 4,000 subsequent measurements to increase the signal-to-noise ratio, thus performing also an averaging over the disorder configurations.

Received 14 December 2012; accepted 22 March 2013; published online 5 May 2013

References

1. Letokhov, V. S. Generation of light by a scattering medium with negative resonance absorption. *Sov. Phys. JETP* **16,** 835–840 (1968).
2. Weaver, H., Williams, D. R. W., Dieter, N. H. & Lum, W. T. Observations of a strong unidentified microwave line and of emission from the OH molecule. *Nature* **208,** 29–31 (1965).
3. Letokhov, V. S. Laser action in stellar atmospheres. *IEEE J. Quantum Electron.* **8,** 615 (1972).
4. Letokhov, V. S. & Johansson, S. *Astrophysical Lasers* (Oxford Univ. Press, 2009).
5. Johnson, M. A., Betz, M. A., McLaren, R. A., Sutton, E. C. & Townes, C. H. Nonthermal 10 micron CO_2 emission lines in the atmospheres of Mars and Venus. *ApJ* **208,** L145–L148 (1976).
6. Mumma, M. J. *et al.* Discovery of natural gain amplification in the 10-micrometer carbon dioxide laser bands on Mars: A natural laser. *Science* **212,** 45–49 (1981).
7. Lavrinovich, N. N. & Letokhov, V. S. The possibility of the laser effect in stellar atmospheres. *Sov. Phys. JETP* **40,** 800–805 (1975).
8. Markushev, V. M., Zolin, V. F. & Briskina, C. M. Luminescence and stimulated emission of neodymium in sodium lanthanum molybdate powders. *Sov. J. Quantum Electron.* **16,** 281–282 (1986).
9. Lawandy, N. M., Balachandran, R. M., Gomes, A. S. L. & Sauvain, E. Laser action in strongly scattering media. *Nature* **368,** 436–438 (1994).
10. Cao, H. *et al.* Random laser action in semiconductor powder. *Phys. Rev. Lett.* **82,** 2278–2281 (1999).
11. Wiersma, D. S. & Cavalieri, S. A temperature-tunable random laser. *Nature* **414,** 708–709 (2001).
12. Wiersma, D. S. The physics and applications of random lasers. *Nature Phys.* **4,** 359–367 (2008).
13. Wiersma, D. S. & Noginov, M. A. Special issue on Nano and random laser. *J. Opt.* **12,** 020201 (2010).
14. Wiersma, D. S. Disordered photonics. *Nature Photon.* **7,** 188–196 (2013).
15. Truitt, P. & Strelnitski, V. Transition to oscillation regime in flaring water vapour masers. *Bull. Am. Astron. Soc.* **32,** 1484 (2000).
16. Labeyrie, G. *et al.* Slow diffusion of light in a cold atomic cloud. *Phys. Rev. Lett.* **91,** 223904 (2003).
17. Labeyrie, G., Delande, D., Müller, C. A., Miniature, C. & Kaiser, R. Multiple scattering of light in a resonant medium. *Opt. Commun.* **243,** 157–164 (2004).
18. McKeever, J., Boca, A., Boozer, A. D., Buck, J. R. & Kimble, H. J. Experimental realization of a one-atom laser in the regime of strong coupling. *Nature* **425,** 268–271 (2003).
19. Guerin, W., Michaud, F. & Kaiser, R. Mechanisms for lasing with cold atoms as the gain medium. *Phys. Rev. Lett.* **101,** 093002 (2008).
20. Vrijsen, G., Hosten, O., Lee, J., Bernon, S. & Kasevich, M. A. Raman Lasing with a Cold Atom Gain Medium in a High-Finesse Optical Cavity. *Phys. Rev. Lett.* **107,** 063904 (2011).
21. Bohnet, J. *et al.* A steady-state superradiant laser with less than one intracavity photon. *Nature* **484,** 78–81 (2012).
22. Schilke, A., Zimmermann, C., Courteille, Ph. W. & Guerin, W. Optical parametric oscillation with distributed feedback in cold atoms. *Nature Photon.* **6,** 101–104 (2011).
23. Froufe-Pérez, L. S., Guerin, W., Carminati, R. & Kaiser, R. Threshold of a random laser with cold atoms. *Phys. Rev. Lett.* **102,** 173903 (2009).
24. Guerin, W., Mercadier, N., Brivio, D. & Kaiser, R. Threshold of a random laser based on Raman gain in cold atoms. *Opt. Express* **17,** 11236–11245 (2009).
25. Guerin, W. *et al.* Towards a random laser with cold atoms. *J. Opt.* **12,** 024002 (2010).
26. Baudouin, Q., Mercadier, N. & Kaiser, R. Steady-state signatures of radiation trapping by cold multilevel atoms. *Phys. Rev. A* **87,** 013412 (2013).
27. Goetschy, A. & Skipetrov, S. E. Euclidean matrix theory of random lasing in a cloud of cold atoms. *Europhys. Lett.* **96,** 34005 (2011).
28. Türeci, H. E., Ge, L., Rotter, S. & Stone, A. D. Strong interactions in multimode random lasers. *Science* **320,** 643–646 (2008).
29. Conti, C. & Fratalocchi, A. Dynamic light diffusion, three-dimensional Anderson localization and lasing in inverted opals. *Nature Phys.* **4,** 794–798 (2008).
30. Dravins, D. in *High Time Resolution Astrophysics* (eds Phelan, D., Ryan, O. & Shearer, A.) 95–132 (Astrophysics and Space Science Library, Vol. 351, Springer, 2008).

Acknowledgements

We acknowledge financial support from ANR (project ANR-06-BLAN-0096), CG06, PACA, DGA and the Research Executive Agency (programme COSCALI, No. PIRSES-GA-2010-268717). We thank R. Carminati and S. Skipetrov for fruitful discussions, and A. Aspect and S. Tanzilli for useful comments on the manuscript.

Author contributions

Q.B., N.M. and V.G. carried out the experiment and analysed the data; Q.B., N.M. and R.K. developed the theory; Q.B., W.G. and R.K. wrote the paper; R.K. supervised the project. Q.B. and N.M. contributed equally to the study. All authors discussed the results and commented on the manuscript.

Additional information

Supplementary information is available in the online version of the paper. Reprints and permissions information is available online at www.nature.com/reprints. Correspondence and requests for materials should be addressed to R.K.

Competing financial interests

The authors declare no competing financial interests.